Towards Quantifying Mesoscale Flows in the Troposphere Using Raman Lidar and Sondes

B. B. Demoz, K. D. Evans, S. H. Melfi, and M. Cadirola
University of Maryland Baltimore County
Baltimore, Maryland

D. O'C. Starr, D. N. Whiteman, and G. Schwemmer
NASA-Goddard Space Flight Center
Greenbelt, Maryland

D. D. Turner
Pacific Northwest National Laboratory
Richland, Washington

R. A. Ferrare
NASA-Langley Research Center
Hampton, Virginia

J. E. M. Goldsmith
Sandia National Laboratories
Livermore, California

Introduction

Water vapor plays an important role in the energetics of the boundary layer processes which in turn play a key role in regulating regional and global climate. It plays a primary role in earth's hydrological cycle, in radiation balance as a direct absorber of infrared radiation, and in atmospheric circulation as a latent heat energy source, as well as in determining cloud development and atmospheric stability. Water vapor concentration, expressed as a mass mixing ratio (g kg^{-1}), is conserved in all meteorological processes except condensation and evaporation. This property makes it an ideal choice for studying many of the atmosphere's dynamic features.

Raman scattering measurements from lidar also allow retrieval of water vapor mixing ratio profiles at high temporal and vertical resolution. Raman lidars sense water vapor to altitudes not achievable with towers and surface systems, sample the atmosphere at much higher temporal resolution than radiosondes or satellites, and do not require strong vertical gradients or turbulent fluctuations in temperature that is required by acoustic sounders and radars.

Analysis of highly resolved water vapor profiles are used here to characterize two important mesoscale flows: thunderstorm outflows and a cold front passage. The data were obtained at the Atmospheric Radiation Measurement (ARM) Cloud and Radiation Testbed (CART) site by the ground-based U.S. Department of Energy (DOE)/Sandia National Laboratories lidar [CART Raman lidar (CARL)] and the Goddard Space Flight Center (GSFC) scanning Raman lidar (SRL). A detailed discussion of the SRL (Ferrare et al. 1995) and CARL (Goldsmith et al. 1998) performance during the intensive observation periods (IOPs) is given by others in this meeting.

Thunderstorm Outflow

Two cases of thunderstorm outflows from the 1994 Remote Cloud Sensing IOP (RCSIOP) are presented. At about 1200 on 27 April 1994, a thunderstorm moved into the CART region from the Texas panhandle and Oklahoma border. Low-level clouds were found (satellite) in advance of the storm. A wind shift, from southwest (SW) to north northeast (NNE), at about 0300 indicated arrival of an "inflow" region over the CART site. The associated low clouds were observed after about 0500.

As evident in the SRL observations (Figure 1), the cloud layer was thin, extending from 1 km to 1.5 km, and exhibited a very flat base. This feature is common to pre-storm environments. Fankhauser (1976) showed that the inflow of an ordinary multicell hailstorm was derived from a layer which, at 20 km ahead of the storm, was restricted to below 1 km above ground level.

Marwitz et al. (1972) also reported that a distinct cloud base associated with an organized updraft can be detected up to 30 km away from an approaching storm. Here, however, the low-level cloud deck extended more than 100 km ahead of the storm and persisted until the storm passed overhead after 1500. In this case, attenuation by the low-level cloud deck limited the SRL observations of water vapor structure at middle and upper-tropospheric levels after 0900. However, the advance of the upper-level moisture and outflow (anvil) is captured by the rawinsonde observations at 1200 (Figure 2). In addition to showing the sub-sounding (less than 3 hr) details of the lower cloud, the SRL reveals atmospheric structure above cloud and details of the boundary layer moisture stratification (drying with time and storm proximity).

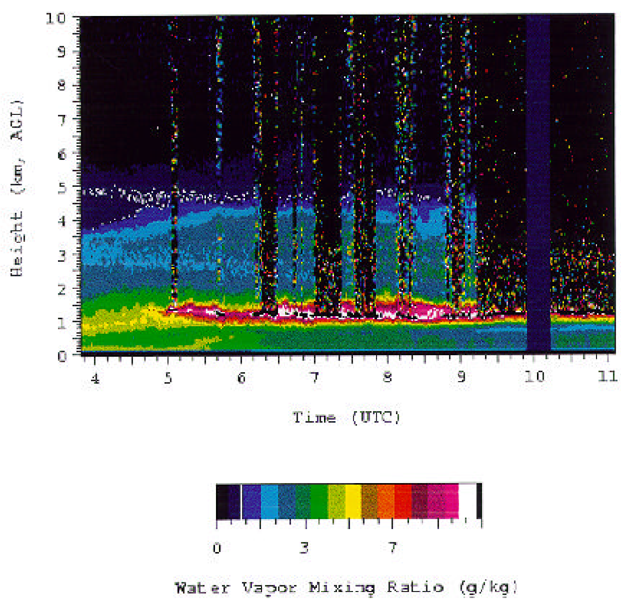

Figure 1. SRL-sensed water vapor mixing ratio (g kg^{-1}) profiles on 27 April 1994 over the CART station. Note the vertical stipling, which indicates attenuation by cloud, and the data gap around 1000. (For a color version of this figure, please see *http://www.arm.gov/docs/documents/technical/conf_9803/demoz-98.pdf*.)

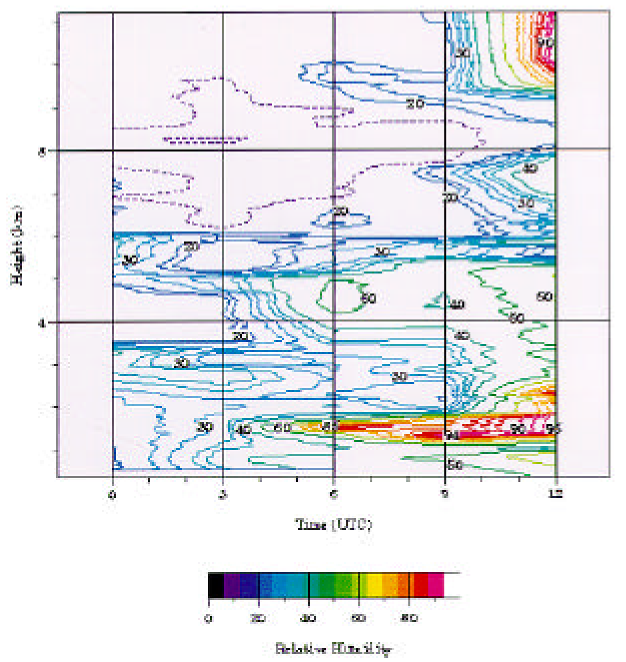

Figure 2. Time-height contour of rawinsonde derived profiles of relative humidity for 27 April 1994. (For a color version of this figure, please see *http://www.arm.gov/docs/documents/technical/conf_9803/demoz-98.pdf*.)

Another example of thunderstorm outflow and anvil clouds is shown in Figure 3. This occurred on 29 April 1994. The low-level moisture was capped by a relatively dry atmosphere. Below about 2 km, wind direction changed from westerly at 0000 to NE and became stronger with time in agreement with thunderstorm inflow observations (Frankhauser 1976). A moist layer at 3 km to 4.5 km, and another in the upper troposphere were detected. The latter agrees well with the expected structure and location of anvil plume formation according to the models of Browning (1977). The anvil (usually composed of broad cirrus shields and mamma clouds) forms as air diverges horizontally in all directions and carries small ice crystals away from the top of the main updraft core into the down-shear direction.

SRL data for this night are shown in Figure 4. This figure is remarkably similar to the soundings, but of much higher resolution. The vertical structure of the continuous decrease in moisture in the lowest 2 km, indicated by the soundings, is well documented. The SRL observations also capture the mid-tropospheric and upper tropospheric moist layers. The anvil moisture plume outflow is shown as a continuously

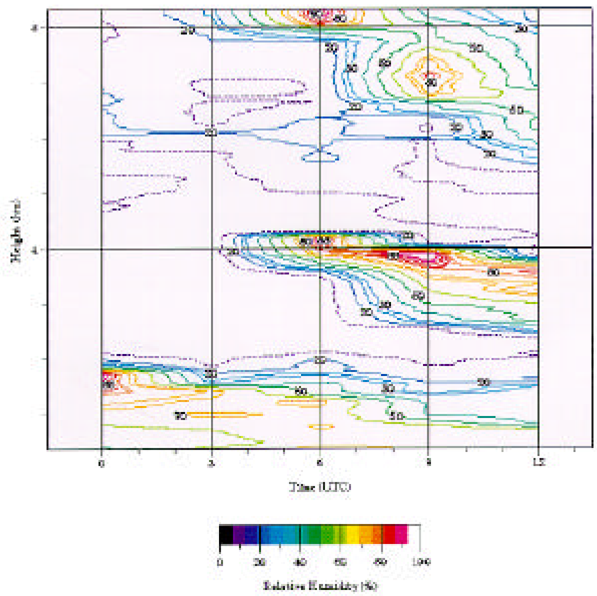

Figure 3. Same as Figure 2, except for 29 April 1994. Note the data gap centered on the 1800 sounding above 6.0 km. (For a color version of this figure, please see *http://www.arm.gov/docs/documents/technical/conf_9803/demoz-98.pdf*.)

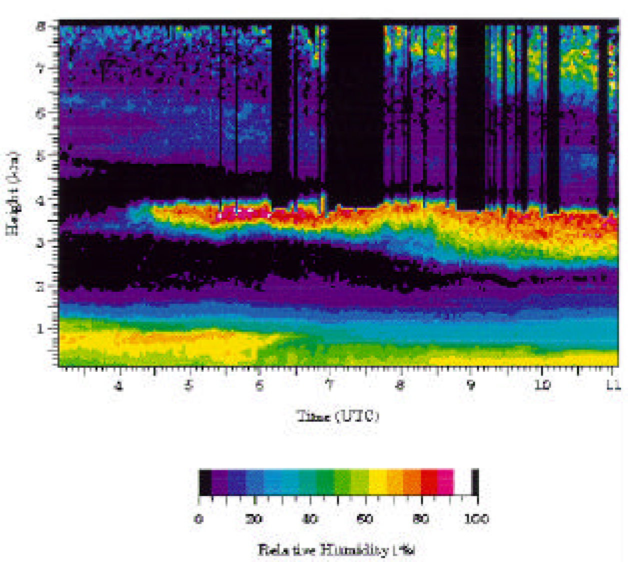

Figure 4. SRL-derived relative humidity (%) profiles on 29 April 1994 over the CART station. The relative humidity is derived using the 3-hr sonde profiles of temperature and pressure. Note the continuously lowering anvil in the upper right corner. (For a color version of this figure, please see *http://www.arm.gov/docs/documents/technical/conf_9803/demoz-98.pdf*.)

lowering base similar to what is often observed by radars, visually. The Pennsylvania State University radar (not shown here) detected the first anvil cloud echo at about 1500, about 4 hr later.

Cloud Base Measurements

A comparison of the SRL-derived cloud base heights (derived using data from the aerosol channel), to those measured by a Belfort laser ceilometer (BLC, usually limited to below 3 km to 4 km) and by a micropulse lidar (MPL; Spinhirne 1993) are shown in Figure 5. This figure shows the excellent correlation between these instruments in detecting cloud base altitudes in both cases. Average cloud base altitudes (km) on 27 April (top figure) were 1.3 (±0.08), 1.15 (±0.07), and 1.15 (±0.07) for the BLC, MPL and SRL aerosol channel, respectively. Altitudes of 80% to 90% relative humidity derived from the SRL water vapor channel data are also shown in Figure 5. These data sets also reveal a moist layer "cloud" at about 7.5 km to 8 km altitude. This is possible because the SRL laser signal is capable of acquiring information above cloud level provided the cloud is not very thick and/or through gaps in the overhead cloud, which was apparently the case. Note that the high altitude moisture detected by the SRL was absent in Figure 2 because the sonde had wandered far from the site. A very good correlation between the instruments is also shown for the 29 April case (lower part of Figure 5).

Average cloud heights (km) of 3.71 (±0.16), 3.79 (±0.09), and 3.96 (±0.11) were detected by the MPL, SRL, and BLC aerosol channel, respectively. The MPL and SRL also show the presence of upper tropospheric clouds with continuously lowering bases until 0700. But, only the SRL detects this moisture associated with the anvil outflow past 0700.

Nonprecipitating Cold Front

Fronts, three-dimensional zones demarcating air masses of different origin and characteristics, are one of the main weather-producing atmospheric structures. As such, considerable effort has been devoted to documenting frontal organization and structure. Most studies of cold fronts use data from rawinsondes, satellite, tower and surface mesonets (dense network of meteorological instruments). Most of these instruments are limited in the information they provide on frontal structure and dynamics. Radars are good at locating clouds and precipitation zones but are unable to provide data in regions where clouds or high concentrations of relatively large aerosols are absent. Tower and acoustic radars do provide valuable data sources in the analysis of

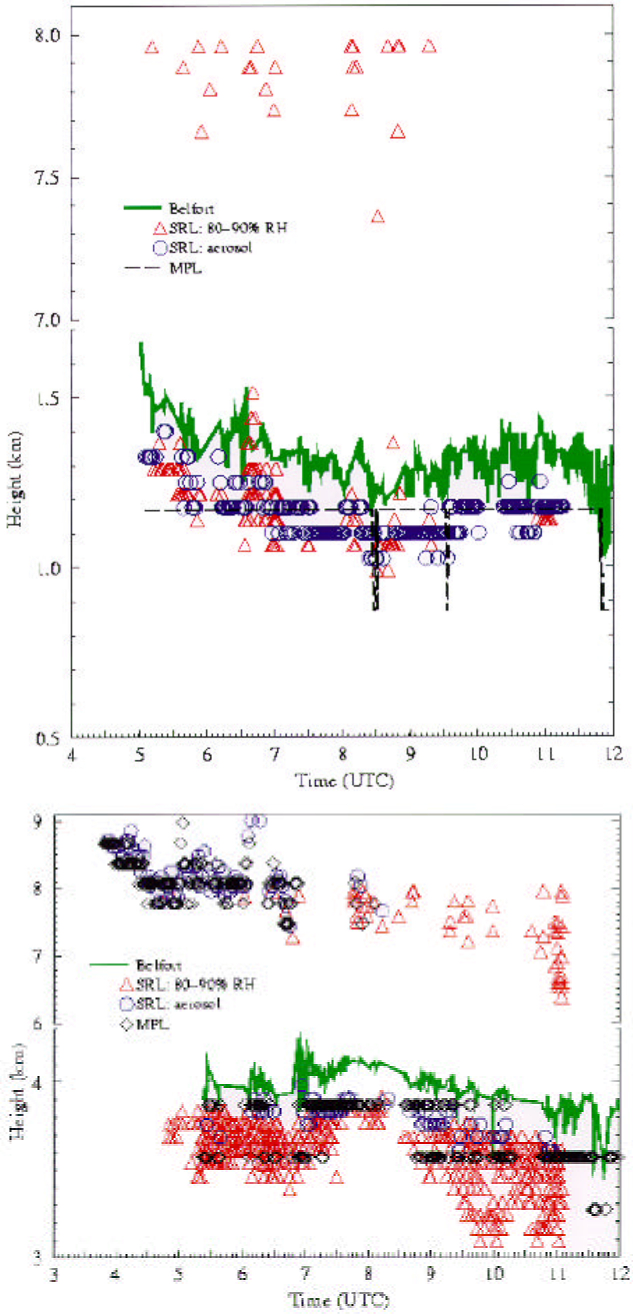

Figure 5. A comparison of cloud base heights derived from measurements made by the SRL aerosol (circle) and water vapor (triangle) channels, BLC (solid line), and the MPL (dotted line) over the CART station on 27 and 29 April 1994. (For a color version of this figure, please see *http://www.arm.gov/docs/documents/technical/conf_9803/demoz-98.pdf*.)

cold front dynamics (Shapiro et al. 1985), but are limited to altitudes of less than about 600 m. Instruments capable of acquiring continuous and high vertical resolution data (e.g., Raman lidar) are required for a detailed study of frontal slope, thickness, cross-front mixing and many other issues. Below, we present analysis of a cold front observed on 28 September 1997 by both the CARL and the SRL.

A contour of relative humidity (Figure 6) derived from the soundings (3 hr) reveals the atmospheric structure, albeit crude, including the moist boundary layer prior to frontal passage (0900) and the drying in post-frontal conditions at low levels. It also shows the saturated elevated layer (cloud) with base at 2.5 km, following the data gap at 0300-0600. This 3-hr resolution of the structure of the atmosphere during the cold frontal passage, however, does not show the fine scale dynamics and structure, nor does it capture any crossfront mixing events that may be taking place. On the other hand, at 75 m vertical and 1 min. to 2 min. temporal resolution, the CARL measured mixing ratio profiles (Figure 7) detail the atmospheric structure to about 8 km altitude. These images of Raman lidar include daylight operation (1200-2400), a recently added advantage. Note that during daytime operation, the signal-to-noise ratio is very low above about 5 km to 6 km.

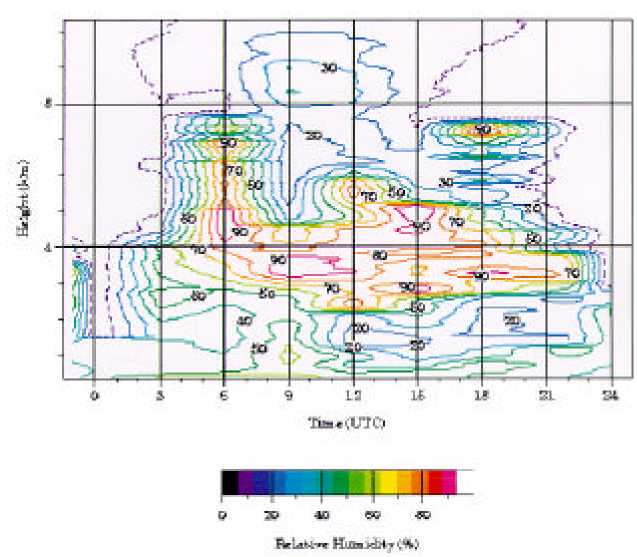

Figure 6. Same as Figure 2, except for 28 September 1997. (For a color version of this figure, please see *http://www.arm.gov/docs/documents/technical/conf_9803/demoz-98.pdf*.)

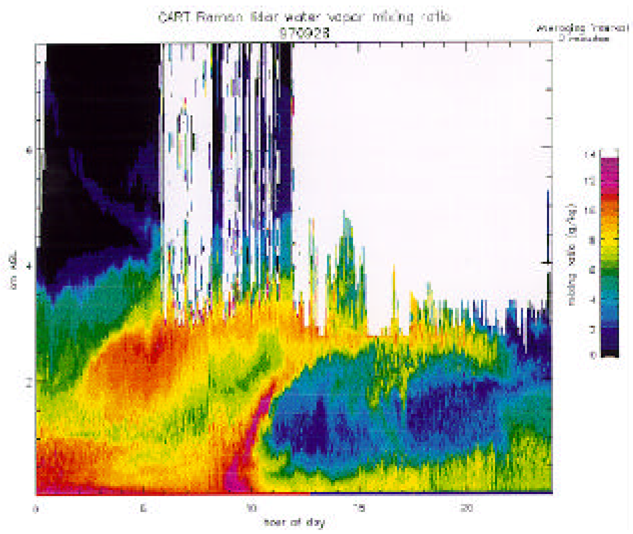

Figure 7. CART Raman lidar-sensed water vapor mixing ratio (g kg^{-1}) profiles on 28 September 1997 over the CART site. Note again that the vertical stipling indicates attenuation by cloud and information is lost above 5 km to 6 km after about 1600 due to low signal-to-noise ratio. (For a color version of this figure, please see *http://www.arm.gov/docs/documents/technical/conf_9803/demoz-98.pdf*.)

The passage of the front at the surface was determined to be a little past 1000, indicated by the drying of the boundary layer to mixing ratios of less than about 4 g kg^{-1}. The leading edge of the cold front resembles the structure of a gravity current (Smith and Reeder 1988) with the leading edge of the front forming a nose-like structure (gravity "head") and buffered from the ground by a slightly moist layer (friction layer). Other interesting features include the elevated moist region (at 2 km to 3 km and around 0500) leading the frontal surface. From Figure 7 and wind profiler measurements (not shown), it was found this moisture originated at near-surface (below mainly about 1 km) and was a back-flow of the airmass that was lifted by the frontal surface. Note that these features and many others cannot be deduced from the 3-hourly soundings or any other conventional meteorological instrument but are readily observed using Raman lidar.

Conclusions

The results shown here demonstrate the Raman lidar system's superb capability in visualizing the detailed vertical and horizontal stratification of the atmosphere to more than 8 km altitude. Fine-scale structures in the boundary layer and/or between air mass boundaries were easily detected and the dynamic processes involved in generating these structures inferred. The water vapor mixing ratio images also compare well to the prevailing conceptual models of fronts or gravity currents and thunderstorm outflows. The moisture "shadow" of the anvil (evaporated and/or sub-visual) is detected well before (3 hr to 4 hr) the presence of ice (detection by radar). Comparisons of cloud base data derived from the SRL, a micropulse laser, and a ceilometer were also in excellent agreement.

References

Ferrare, R. A., S. H. Melfi, D. N. Whiteman, K. D. Evans. F. J. Schmidlin, and D. O'C. Starr, 1995: A comparison of water vapor measurements made by Raman lidar and radiosondes. *J. Atmos. Oceanic Technol*., **12**, 1177-1195.

Browning, K. A., 1977: The structure and mechanisms of hailstorms. *Meteor. Monogr*., **38**, 1-43.

Fankhauser, J. C., 1976: Structure of an evolving hailstorm, Part 11: Thermodynamic structure and airflow in the near environment. *Mon. Wea. Rev*., **104**, 576-587.

Goldsmith, J. E. M., F. H. Blair, S. E. Bisson, and D. D. Turner, 1998: Turn-key Raman lidar for profiling atmospheric water vapor, clouds, and aerosols. *Applied Optics*, in press.

Marwitz, J. D., A. H. Auer, and D. L. Veal, 1972: Locating the organized updraft on severe thunderstorms. *J. Appl. Meteor*., **11**, 236-238.

Shapiro, M. A., T. Hampel, D. Rotzoll, and F. Mosher, 1985: The frontal hydraulic head: A meso-a scale (1 km) triggering mechanism for mesoconvective weather systems. *Mon. Wea. Rev*., **113**, 1166-1183.

Smith, R. K., and M. J. Reeder, 1988: On the movement and low-level structure of cold fronts. *Mon. Wea. Rev*., **113**, 1166-1183.

Spinhirne, J. D., 1993: Micro pulse lidar. *IEEE Trans*, **31**, 48-55.